ISSN: 1813-162X (Print) ; 2312-7589 (Online)

Tikrit Journal of Engineering Sciences

available online at: http://www.tj-es.com

Effects of Rice Husk Ash–Magnesium Oxide Addition on Wear Behavior of Aluminum Alloy Matrix Hybrid Composites

Abbas Y. Awad [1, *]

Mohammed N. Ibrahim[1]

Mohamed K. Hussein[2]

[1] Directorate of Materials Research
Ministry of Science and Technology
Baghdad, Iraq

[2] Engineering Technical College-Baghdad
Middle Technical University
Baghdad, Iraq

***Keywords*:**

Aluminum hybrid composites
rice husk ash
magnesium oxide
stir casting

ARTICLE INFO

Article history:

Received xx September 201x
Accepted xx March 201x
Available online xx June 201x

ABSTRACT

A336.0 aluminum alloy used to fabricate hybrid composites using rice husk ash (RHA) and MgO particles as reinforcement. The influence of the particles on the wear behavior of A336.0 aluminum alloy as a matrix that reinforced with MgO and RHA was investigated. Firstly, the rice husk burned at 700°C and then heat treated at 1100°C for 2 hrs. The ash characterized by X-ray florescence and X-ray diffraction. Less than 53 and 125 micron are the particle sizes of MgO and RHA respectively. The hybrid composites manufactured using stir casting method in two steps. A336.0 aluminum alloy reinforced with 4:0, 3:1, 2:2, 1:3 and 0:4 of RHA: MgO with 10 wt% total reinforcement phase. Optical microscope and X-ray diffraction were used to characterize the prepared hybrid composites. Dry sliding wear, hardness, apparent density, percentage of porosity and coefficient of friction were examined. Results indicated that porosity, apparent density and hardness enhanced with increasing MgO, while increasing wt% of RHA decreased the apparent density. Results indicated that with inceasing the applied load the wear rate of the composites was enhanced. Coefficient of friction varies inversely with applied load and wt% of RHA. Hardness increased with increasing RHA while the friction coefficient and the wear rate decreased. The minimum wear rates were at 10% RHA and Al-alloy-(RHA-MgO) [3:1] composites, while the minimum friction coefficients were at 10% RHA composites.

DOI: http://dx.doi.org/10.25130/tjes.25.x.0x

تأثير إضافة رماد قشور الرز – اوكسيد المغنسيوم على سلوك البلى لمواد متراكبة هجينة ذات أساس من الألمنيوم

الخلاصة

تم استخدام سبيكة ألمنيوم نوع A336.0 لتحضير مادة متراكبة باستخدام رماد قشور الرز (RHA) مع اوكسيد المغنسيوم (MgO) كمواد تقوية. اجريت دراسة تأثير الدقائق المضافة على سلوك البلى للمادة المتراكبة الناتجة. تم تحضير الرماد بحرق قشور الرز عند 700 مئوي ثم اجراء معاملة حرارية للرماد المتكون عند 1100مئوي ولمدة ساعتين بعدها اجريت فحوصات للرماد لتحديد كمية الاكاسيد باستخدام الاصدار الفلوري للاشعة السينية (XRF) وكذلك استخدام حيود الاشعة السينية (XRD) لتحديد الاطوار المتكونة. حجم دقائق المسحوق لكل من اوكسيد المغنسيوم والرماد كانت اقل من 53 و125 مايكرون على التوالي. عملية الانتاج كانت باستخدام طريقة الدوامة على مرحلتين لخلط RHA: (MgO) مع منصهر سبيكة الالمنيوم وبنسب وزنية (4:0, 3:1, 2:2, 1:3, 0:4) لنسبة خلط كلية 10%. تم اختبار كل من الصلادة، معدل البلى، معامل الاحتكاك، النسبة المئوية للمسامية والكثافة الظاهرية بالإضافة الى اجراء اختبار حيود الاشعة السينية والفحص المجهري لعينات المتراكبات الناتجة. اظهرت النتائج ان زيادة نسبة اوكسيد المغنسيوم يزيد من نسبة المسامات والكثافة الظاهرية بالإضافة الى رفع صلادة المركبات الناتجة، حيث عند 10% من اوكسيد المغنسيوم ستزداد المسامات لأعلى مستوى وتقل الكثافة. كما تبين ان الصلادة تزداد مع زيادة نسبة الرماد بينما يقل معدل البلى ومعامل الاحتكاك. لوحظ ايضا ان معامل الاحتكاك يتناسب عكسيا مع ازدياد نسبة الرماد والحمل المسلط. اقل معدل بلى كان عند العينة RHA%10 والعينة [3:1] (RHA: MgO)، بينما اقل معامل احتكاك كان عند العينة RHA%10.

1. INTRODUCTION

In recent years, different recycled wastes are used to improve a specification of composites. There are various reinforcement fillers used, among the agricultural residue that abundantly available is the rice husk ash [1]. Waste materials can be used to reinforce composites, increase the mechanical properties and reduce the cost in addition to clean the environmental residue [2]. Recently, researchers

* *Corresponding author: E-mail* : abbas_yass@yahoo.com

are trying to increase performance of composites to meet the demand that represented by lightweight, corrosion resistance, wear and environmental friendly [3]. The overall properties of conventional aluminum alloy are lower than aluminum matrix composites (AMCs). There are several advantages of aluminum matrix composites compared with unreinforced alloys represented by high strength, high stiffness, reduced density (weight), enhanced high temperature properties such as thermal expansion, enhanced damping capabilities and increased abrasion and wear resistance [4]. Isotropic properties and relatively minimum cost of aluminum matrix composites that used particulate as a reinforcement materials are attractive for researching [5]. Hybrid composites are relatively new materials that manufactured using more than two different types of reinforcements. The composites that include only a single reinforcement phase possess lower properties compared with the hybrid types [6]. Proportions of the reinforcement and the matrix in addition to properties of them are the main factors which control isotropy of the system, microstructure, homogeneity and volume fraction that determine the properties of composites. Stir casting process possess many advantages that represented by flexibility, applicability to large quantity production and simplicity. This process is suitable as economic method to manufacture metal matrix composites [7]. Up to 30% volume fractions of reinforcements, stir casting process is suitable to manufacture composites [8]. Prasad et al. [9] used SiC and RHA in various fractions to fabricate aluminum composites using double stir casting process. It was observed that with increasing reinforcement percentage, the density decreases, while the porosity and hardness of the hybrid composites increased. Balaji et al. [10] reinforced Al 6061- alloy with different wt. % of MgO to study the mechanical properties of the composite. Wear resistance, compressive strength and hardness of the matrix alloy are lower than the composites. Dry sliding wear of Al/RHA composites that manufactured using stir casting process was studied by Pydi et al. [12]. The results showed that the friction coefficient and wear rates of aluminum composites various inversely with RHA wt% and the wear resistance of Al/RHA composites is higher than unreinforced aluminum. A356.2 / RHA composites manufactured using stir casting method with different weight fractions of reinforcement by Prasad and Krishna, [13]. Many mechanical properties of the composites were increased with increasing percentage of RHA while the density decreased. This work aimed to study the effects of RHA and MgO additions on the wear rate of the hybrid composites and determine the optimum RHA: MgO weight ratios to get better performance of the composites.

2. MATERIALS AND METHODS

2.1. Materials

A336.0 Aluminum alloy (ASM, 1992) as a matrix alloy used for composites manufacture. Used mini bus pistons that available in the local market used as the source of aluminum alloy. Spectrometer type (ARL 3460, USA) used to analysis the chemical composition of pistons as shown in Table 1.

Table 1
Chemical composition of Al-alloy bus piston.

Elements	Standard alloy	Actual alloy
Si	11-13.5	12.5
Cu	0.5-1.3	1.19
Mg	0.8-1.3	0.8
Fe	1.0 max	0.5
Ni	0.5-1.3	0.5
Zn	0.25 max	0.08
Cr	0.1 max	0.01
Al	Bal.	Bal.

2.2. Preparation of Master Aluminum Alloy

Small pieces of the used pistons were cleaned using emery paper No. 240 and then melted using gas fired furnace in alumina crucible. Firstly, the furnace was heated to 750 °C for 30 minutes to ensure complete melting of the alloy. K-type thermocouple was used to measure the temperature of molten alloy. 1wt % of aluminum chloride (AlCl3-6H2O) and 1wt % of sodium chloride were added to degas the molten alloy. Al-alloy castings prepared using a cylindrical carbon steel mold. The master alloy that used as the matrix for composites was taken from these ingots (d = 15 mm, h = 150 mm).

2.3. Preparation of RHA

Firstly, the rice husk was washed in a stainless steel container with a tap water several times after it blown manually. Stainless steel trays used to sun dried of the washed rice husk for 24 hrs. The rice husks were burned using a cylindrical steel container (h = 20 cm and d = 75 cm). Kerosene as a fire source used to burn the rice husk for 3 hrs and then left the ash to cool down for 12hrs. The ash sieved to 125 micron after complete burning process. The ash was heat treated at 1100 °C for 2 hrs to remove the carbonaceous materials using electrical furnace with a heating rate of 7˚C/ min and then furnace cool. The ash that burned at 700 °C has black color, while grayish white color of the heat treated ash, as shown in Fig. 1.

(a) (b)

Fig. 1. (a) RHA burned at 700 °C; (b) RHA heat treated at 1100 °C for 2 hrs

2.4. Al- Alloy/ RHA-MgO Hybrid Composite Preparation

Stir casting process was used to cast 500 gm of composite materials for each time. 445 gm of Al- master alloy, 50 gm of (RHA: MgO) powder with various ratios and 5 gm of magnesium flakes (99% purity, England) as

shown in Table 2. The aluminum alloy was heated to 750°C for 30 minutes to ensure homogeneity of molten alloy using gas fired furnace and to improve the wettability, magnesium was used [13]. The powders preheated to 350°C to remove the moisture and to enhance the stacking with molten alloy [14]. At 675 °C, the magnesium was added to the molten alloy. Two batches of both preheated powders were added to the molten alloy at 630 °C. The temperature of molten alloy was reduced to 590 °C after addition of the first batch and stirred manually for 3 minutes. The mixture of powders and molten alloy heated to about 630- 640 °C and then second batch was added and stirred manually for 3-4 minutes. The temperature was increased to 780 °C after completed of the manually mixing process and then stir the mixture for 4-5 minutes using stainless steel mixer at speed 500-600 rpm. At 590 °C, the mixture becomes semi-solid state with high viscosity and that helps to break the gas layer by the abrasive action. At 760 °C, the mixture poured into a preheated cylindrical mold (d = 15 mm, h = 160 mm) of carbon steel to 350 °C. Samples for hardness, microstructure and wear test were fabricated from these ingots after it cooled to room temperature.

Table 2
Al-alloy/ RHA-MgO composite.

Sample number	Composition
1	Al-alloy
2	Al-alloy+10% RHA+0%MgO
3	Al-alloy +7.5% RHA+2.5%MgO
4	Al-alloy + 5%RHA+5% MgO
5	Al-alloy +2.5% RHA+7.5%MgO
6	Al-alloy+ 0%RHA+10%MgO

2.5. Hardness Test

According to ASTM E384 standard [15] the samples of the hybrid composites were prepared. The hardness test carried out using micro-vickers hardness machine (Model: HVS-1000, USA manufacture). The samples that used for hardness test had a cylindrical shape with height 10 mm and 12 mm of diameter. 490 gm of the applied load used for 20 seconds to carry out the test and then five hardness readings as average were taken. This average used to calculate the HV according to the following relation [15]:

$$Hv = 1.854 \left(\frac{P}{d2}\right) \quad (1)$$

where
P: applied load (kgf)
d: arithmetic mean of the two diagonals, d1 and d2 in mm.

2.6. Wear Rate and Coefficient of Friction Measurement

Wear test samples prepared according to ASTM G99-95 standard [15]. A pin-on-disc apparatus (Model: ED-201, India) used to measure the wear rate of the hybrid composites and frictional force. At room temperature, the wear tests carried out using 5, 10, 15 and 20 N for 15 minutes. The track diameter of steel disc that used to hardness test was 60 mm with sliding speed 480 rpm and 62HRC hardness. Fixed time period was used to carry out the wear test and then the sample weighed after cleaned with alcohol and dried. According to the following relation, the wear rate calculated using the mass loss method [16]:

$$WR = \frac{\Delta m}{2\pi r n t} \quad (2)$$

where
WR: wear rate, (gm/cm).
Δm: mass lost (gm) which is the difference in mass of the specimens before and after every test.
t: sliding time, (minutes).
r: the radius of the specimen to the center of the disc, (cm).
n: disk speed in rpm.

The coefficient of friction was computed from the applied load and the recorded frictional force. The coefficient of friction (μ) can be defined depending on Amonton's law:

$$\mu = \frac{F}{N} \quad (3)$$

where
F: frictional force, (N)
N: the normal force (force perpendicular to the horizontal surface, which is essentially the weight of the object).

2.7. Apparent Density and Porosity Measurements

Archimedes principles (ASTM C373-88) [17] used to calculate the porosity and apparent density. ∓0.1 mg is the accuracy of the digital balance type Sartorius (model: BL 210 S, Germany) that used to weigh the composite samples. Accordance to the following relation, the apparent density calculated experimentally [18]:

$$\rho a = \left(\frac{Wa}{Wa - Ww}\right) \times \rho w \quad (4)$$

where
Wa: weight of sample in air, (g)
Ww: weight of sample in water, (g)
ρa: apparent density of composite, (g/cm³)
ρw: density of water, (g/cm³)

Porosity must be kept to a minimum to elevate the mechanical properties of the samples. Porosity cannot be fully removed during the casting process, but it can be reduced [19]. According to the following relation, the percentage of porosity evaluated [20]:

$$\%\text{Porosity} = \left(\frac{\rho_{\text{th}} - \rho_{\text{exp}}}{\rho_{\text{th}}}\right) \times 100\% \quad (5)$$

where
ρ_{th} and ρ_{exp} are the theoretical and experimental density (g/cm³), respectively.

2.8. Microstructural Examination

Optical microscope (Model: MT 71000, Japan) with a digital camera (canon, Japan) used to determine the microstructure of the composites. Sample washed with alcohol and dried after it ground and polished and then etched using Keller's reagent (95 ml water, 1.0 ml HF, 1.5 ml HCl, 2.5 ml HNO3) for 15 seconds [21].

2.9. X-Ray Florescence and XRD

The amount of oxides and elements in the RHA determined using X-ray florescence type Spectro / Ametek, (model: XEPOS, Germany), while XRD type Shimadzu (model: XRD-6000, Japan) used to determine the phases of the ash. The shape of the sample is cylindrical with 10mm of diameter and 10 mm of height that used for XRD. The type of material tested is determining the angle range of the diffractrometer that has wave length 1.54060 A°. 5°/min is the speed of the scanning process and the testing angle ranged from 10° to 80°.

3. RESULTS AND DISCUSSION

3.1. Rice Husk Ash Characterization

The chemical composition and XRD of RHA that was treated at 1100 °C for 2 hrs are shown in Table 3 and Fig. 2, respectively. Silica with purity (91%) is the main oxide in RHA, while carbon and other inorganic oxides are available in small amounts. Main silica phases are represented by cristobalite and tridymite in XRD patterns. Firstly, porous and amorphous silica was available, but it changed to crystalline structure after the heat treatment. This result in agreement with investigates of Ramezanianpour et al. [22]. Generally, at a temperature above 500 °C, the rice husk ash changes from purely amorphous to crystalline phase [23].

Table 3
Chemical composition of RHA.

Element	Wt%
SiO_2	91
C	4.7
CaO	2.54
Fe_2O_3	0.65
Na_2O	0.58
MgO	0.25
K_2O	0.123
others	< 0.1

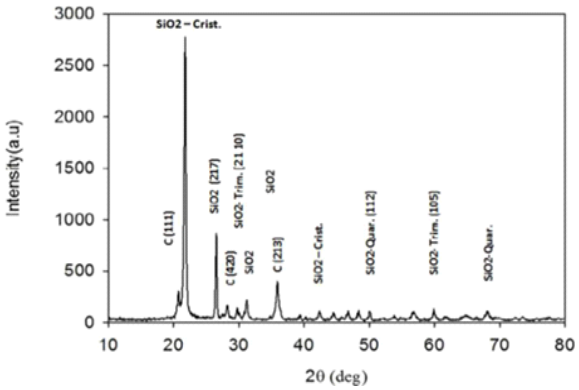

Fig. 2. XRD of heat treated RHA.

3.2. Microstructure of Al- Alloy Composites

A mixture of aluminum and primary silicon in addition to eutectic phase are represented by the microstructure of Al- master alloy as shown in Fig. 3(a). The grains of Al- alloy-RHA composite had coarsening as shown in Fig. 3(b) due to the coarse nature of the ash. Fig. 3(c) shows the finer dendrite arm and more uniform distributed of the reinforcement particles in the microstructure of Al- alloy-MgO composite that had MgO rich eutectic phase. The finer MgO particles are act in the solidification process as nuclei for the grain formation and these particles agglomerated between the dendrite arms with progress of the solidification. Fig. 3(d) shows the microstructure of Al- alloy-(RHA-MgO) [2:2] composite that had finer dendrites compared with Al- alloy-RHA. During liquid matrix alloy solidification, the reinforcement particles may engulf or ejected near the freezing front, where it migrates away from the freezing front [19].

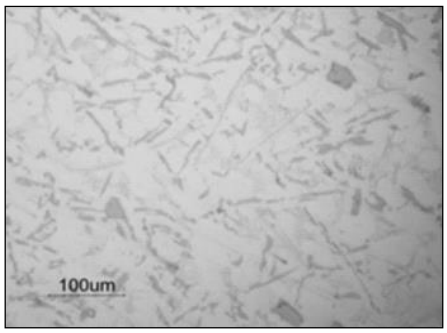

(a) Al-master alloy.

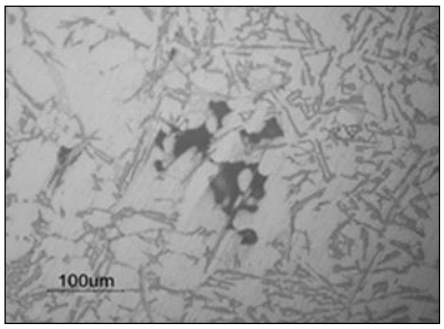

(b) Al- alloy-10% RHA.

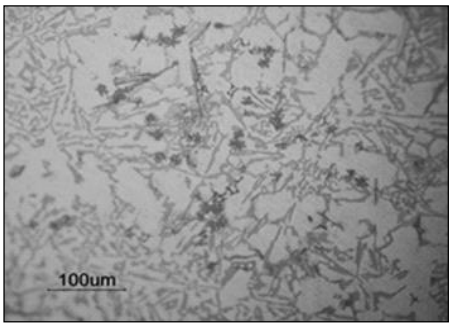

(c) Al- alloy- 10% MgO

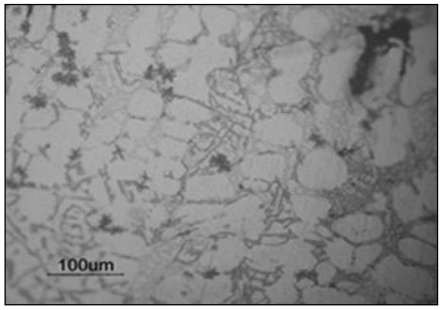

(d) Al- alloy-(5%RHA- 5%MgO)

Fig. 3. Microstructure (a) Al-master alloy, (b) Al- alloy-RHA composite, (c) Al- alloy-MgO composite and (d) Al- alloy-[5% RHA- 5% MgO] hybrid composite.

3.3. X-Ray Characterization

Fig. 4 shows the XRD patterns of Al-master alloy that include three distinct peaks of Al, Si and $FeAl_2$ phases. The main phase was Al and the minor phases represented by $MgAl_2O_4$, Al_8Fe_2Si and Al_2CuMg. XRD pattern of Al-alloy-RHA revealed Al and Si in addition to other minor distinct peaks represented by carbon, SiO_2, Al_8Fe_2Si and $Mg_2Al_4Si_5O_{18}$ phases as shown in Fig. 5. XRD of Al- alloy-MgO that shown in Fig. 6 revealed some minor phases represented by MgO and Al_3Mg_2 with the main phases represented by Al and Si. Some Intermetallic compounds such as Al_3Mg_2 phase that formed because of the addition of Mg to the Al-alloy matrix.

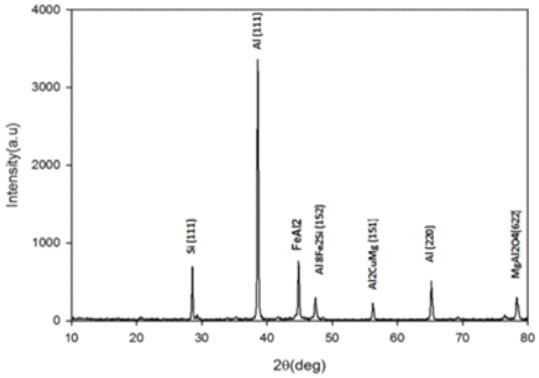

Fig. 4. XRD of Al-master alloy.

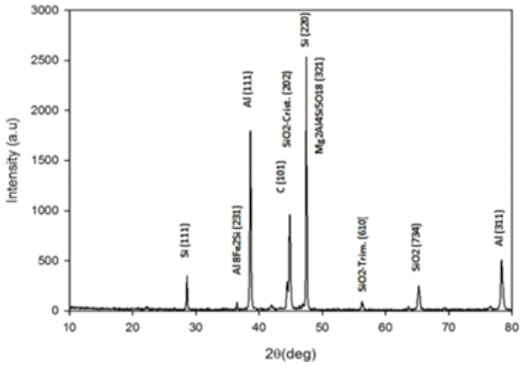

Fig. 5. XRD of Al-alloy-RHA composite.

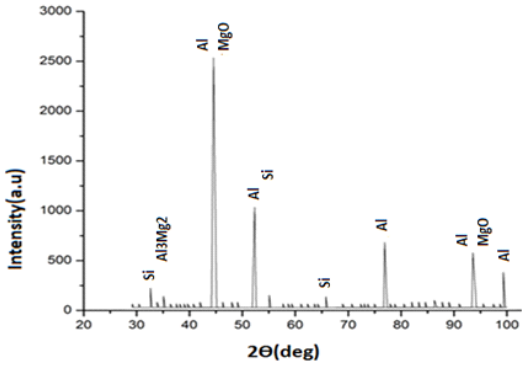

Fig. 6. XRD of Al-alloy-MgO.

3.4. Hardness of Hybrid Composites

Micro hardness performed under 490 gm load and 20 second duration time. Hardness values changed with changing the type and amount of fillers in samples as shown in Fig. 7. Addition of the rice husk ash reinforcement increased the hardness by increasing the amount of the hard and brittle phase in the matrix and that lead to increase the dislocation density at the matrix - particles interfaces as reported by [24]. Hardness of the composites increased with increasing the finer powder represented by MgO in the matrix. The increase in hardness was due to prohibiting of Al grain growth during solidification and enhancement the density of the dislocations [25].

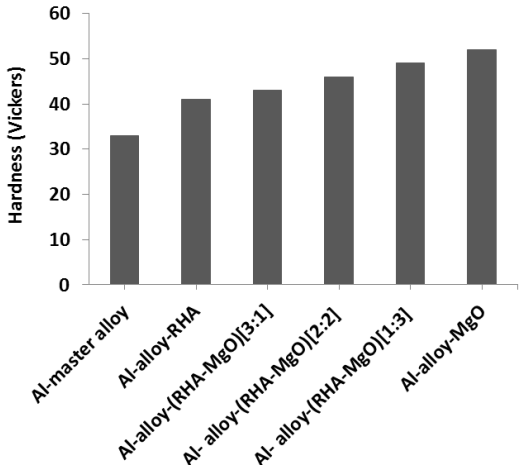

Fig. 7. Hardness of Al-master alloy, Al- alloy-(RHA-MgO) hybrid composites.

3.5. Apparent Density and Porosity of Al-Alloy-(RHA-MgO)

The measured density of Al-master alloy was 2.632 g/cm³, while the other samples of composites possess different values with changing of filler content as shown in Table 4. Measured density of the hybrid composites increased with increasing content of MgO percentage in the reinforcement

Table 4
Density and porosity of Al-master alloy and Al- alloy-(RHA-MgO) hybrid composites.

Sample	Composition	Theoretical density (g/cm³)	Apparent density (g/cm³)	Porosity (%)
1	Al -master alloy	2.71	2.632	2.87
2	Al- alloy-RHA composite	2.61	2.53	3.06
3	Al- alloy-(RHA-MgO) [3:1] hybrid composite	2.656	2.628	1.05
4	Al- alloy-(RHA-MgO) [2:2] hybrid composite	2.7	2.665	1.29
5	Al- alloy-(RHA-MgO) [1:3] hybrid composite	2.74	2.7	1.46
6	Al- alloy-MgO composite	2.762	2.67	3.3

phase (RHA: MgO). At a weight ratio of (1:3) of RHA: MgO, the hybrid composites had higher measured density

due to high density value of MgO compared with Al alloy. At 10% MgO, the measured density decreased due to decrease the wettability with molten alloy and increase the agglomeration with increasing of powder amount and that elevated the porosity content. The measured porosity of Al-master alloy is 2.87%, while the other samples had different values with different filler content. The air envelope of the particles and gas entrapment during stir casting and solidification in addition to hydrogen evolution increased the porosity [10]. The higher percentage of nonmetal particles encourage the nucleation of bubbles in the composite and that lead to elevate porosity content as reported by Hashim et al. [19].

3.6. Wear Behavior

The results revealed that with increasing the applied load, the wear rate of the hybrid composites and Al-master alloy increased as shown in Figure 8. This increment in wear rate can be attributed to generate more heat due to increase in friction between the mating surfaces and that will causes localized welding and then shearing of welded interfaces in addition to increasing the ability of fracture particles (debris) to penetrate the surface. The removal of material from the surfaces is influenced by three-body system between sample and disk surfaces that formed with availability of the fracture particles [26,27]. Generally, the composites had lower wear rate compared with the master alloy. These results due to increasing the hardness of the composites that came from reinforcement's particles in the matrix and that compatible with the work of Prasad and Krishna [28]. The graphite in the ash (as confirmed by XRD) formed a solid lubricant layer that minimize the wear rate of Al- alloy-RHA compared with Al- alloy- MgO composite and that compatible with the work of Kumar et al. [29]. Al-alloy-(RHA-MgO) [3:1] hybrid composite had minimum wear rate compared with other hybrid composites. This result due to reduce the actual contact area and endure the applied load by the ash particles in addition to the lubricating property of graphite as reported by Sharma et al. [26]. The wear rate of composite is increased with increasing percentage of MgO as shown in Fig. 8(b). The mean size and number of fracture particles increased with increasing amount of MgO due to increase the percentage of porosity in the composite. At 10% MgO, the wear rate had minimum values for all loads due to increase the hardness of the composites. Al-alloy-(RHA-MgO) [1:3] had maximum wear rate compared with other hybrid composites due to higher percentage of porosity, where the adhesive wear and delamination increased with increasing the applied load, while Al-alloy-RHA composite had minimum wear rate.

3.7. Coefficient of Friction (COF)

At different loads 5, 10, 15 and 20 N, the coefficient of friction studied with varying percentage of reinforcement particles as shown in Fig. 9. At beginning, the COF had higher values at low load (5 N) due to interlocking of the surfaces and that required higher frictional force to slide the surfaces. As a result of abrasion and formation of a transfer film, the contact surfaces

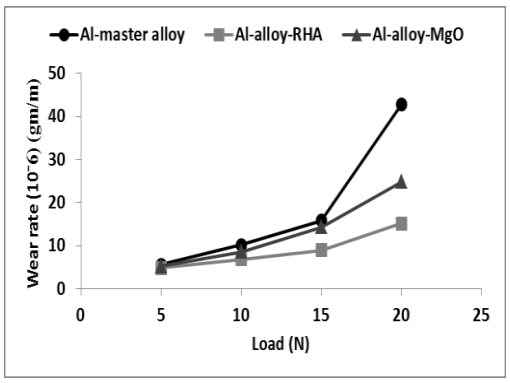

(a)

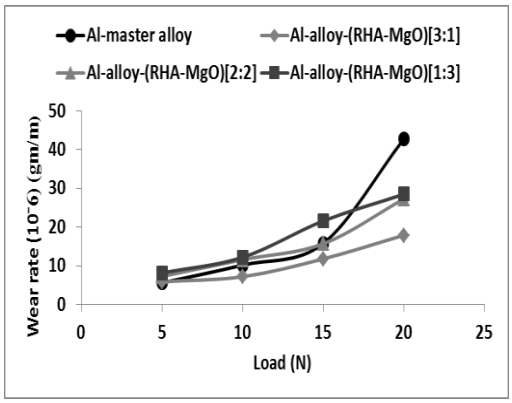

(b)

Fig. 8. Wear rate (a) Al-master alloy, Al- alloy-RHA and Al-alloy-MgO composites, and (b) Al-master alloy, Al-alloy-(RHA-MgO) hybrid composites.

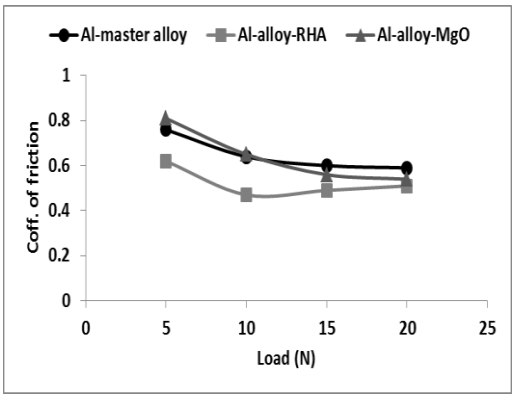

(a)

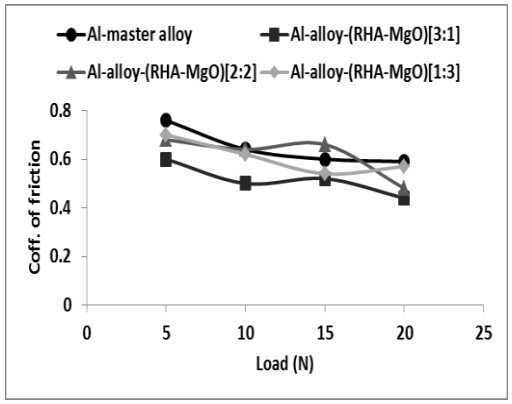

(b)

Fig. 9. COF (a) Al-master alloy, Al- alloy-RHA and Al-alloy-MgO composites, and (b) Al-master alloy, Al-alloy-(RHA-MgO) hybrid composites.

become smoother at higher load and continuing the wear process [30]. Al-master alloy had higher coefficient of friction than Al- alloy composites at 5 N that can be attributed to absence of tribo layer formation of the master alloy and increasing the contact area between two surfaces [26]. The reinforcement particles restricted the flow of metal during sliding with increasing the applied load and act as load bearing members and that lead to decrease the actual contact area between the disk and sample surfaces. These reasons decreased the COF of the composites as reported by Singh et al. [31] who proved that a temperature of aluminum matrix alloy is higher than aluminum composites irrespective of applied force and the surface conditions.

Plastic flow of materials increases with increasing of the applied load due to softening the materials at the specimen interface with elevated temperature. At all loads, 10%RHA composite possess the lowest COF due to smearing the graphite layer [28]. Generally, the COF of the composites and the master alloy decreased with increasing of the applied load except for Al- alloy-(RHA- MgO) [2:2] hybrid composite at 15 N due to formation of tribofilm at the interface between the contact surfaces [32].

4. CONCLUSIONS

1. The composites possess higher value of hardness due to the reinforcement particles compared with the matrix alloy.
2. The hardness of composites increased with increasing percentage of MgO in the reinforcing phase (RHA: MgO) and at 10 wt% of MgO, the hardness reached to the maximum value.
3. Al- alloy-10 %RHA composite had minimum wear rate compared with other composites.
4. The coefficient of friction varies inversely with volume fraction of RHA and the applied load.
5. The reinforcement phase (RHA: MgO) increased the amount of porosity to reach its highest value at 10wt% of MgO, while (RHA-MgO) [3:1] hybrid composite had lower value of porosity.
6. With increasing content of MgO, the measured density increases and then decreased at 10wt% of MgO because of increase percentage of porosity.
7. Addition of MgO leads to form intermetallic compounds and refinement of the microstructure, while the coarse nature of RHA ash increased the grain size of the composites.

REFERENCES

[1] Saravanan S, Kumar MS. Effect of mechanical properties on rice husk ash reinforced aluminum alloy (AlSi10Mg) matrix composites. *Procedia Engineering* 2013; **64**: 1505-1513.

[2] Senapati AK, Sahoo PK, Singh A, Dash S, Manas VS. A review on utilization of waste material as reinforcement in MMCs. *International Journal of Research in Advent Technology* 2015; **3** (5): 15-20.

[3] Subrahmanyam A, Narsaraju G, Rao BS. Effect of rice husk ash and fly ash reinforcements on microstructure and mechanical properties of aluminium alloy (AlSi10Mg) matrix composites. *International Journal of Advanced Science and Technology* 2015; **76**: 1-8.

[4] Suresh S, Mishra D, Srinivasan A, Arunachalam R, Sasikumar R. Production and characterization of micro and nano Al2O3 particle-reinforced LM25 Aluminium alloy composites. *Journal of Engineering and Applied Sciences* 2011; **6** (6): 94-97.

[5] Kala H, Mer K, Kumar S. A review on mechanical and tribological behaviors of stir cast aluminum matrix composites. *Procedia Materials Science* 2014; **6**: 1951-1960.

[6] SA BR, Swamy A, Ramesh A. Mechanical and tribological behavior of aluminum metal matrix composites using powder metallurgy technique- a review. *International J of Mechanical Engineering and Robotics Research, India* 2014; **3** (4): 551-563.

[7] Mathur S, Barnawal A. Effect of process parameter of stir casting on metal matrix composites. *International Journal of Science and Research* 2013; **2** (12): 395-398.

[8] Subramani N, Balamurugan M, Vijayaraghavan K. Mechanical behavior of Al-SiC composites prepared by stir casting method. *International Journal of Innovative Research in Science, Engineering and Technology, India* 2014; **3** (3): 10467-10473.

[9] Prasad DS, Shoba C, Ramanaiah N. Investigations on mechanical properties of aluminum hybrid composites. *Journal of Materials Research and Technology* 2014; **3** (1): 79-85.

[10] Balaji P, Arun R, JegathPriyan D, Ram IM, Manikandan E. Comparative study of Al 6061 alloy with Al 6061–magnesium oxide (MgO) composite. *International Journal of Scientific & Engineering Research* 2015; **6** (4): 408.

[11] Alaneme KK, Olubambi PA. Corrosion and wear behaviour of rice husk ash-Alumina reinforced Al–Mg–Si alloy matrix hybrid composites. *Journal of Materials Research and Technology* 2013; **2** (2): 188-194.

[12] Pydi HP, Prasad Saripalli H, Abburi M, Murthy B, Sivaprasad D. Scanning electron microscope studies on dry sliding wear behaviour of metal matrix composites with Aluminium and rice husk ash. *International Journal of Integrative Sciences, Innovation and Technology* 2012; **1** (2): 1-5.

[13] Prasad DS, Krishna AR. Production and mechanical properties of A356. 2/RHA composites. *International Journal of Advanced Science and Technology* 2011; **33**: 51-58.

[14] Alaneme KK, Adewale T. Influence of rice husk ash–silicon carbide weight ratios on the mechanical behaviour of Al-Mg-Si alloy matrix hybrid composites. *Tribology in Industry* 2013; **35** (2): 163-172.

[15] John B, John B, Peter B. ASM handbook Volume 8: mechanical testing and evaluation: ASM International; 2017.

[16] Prasad N, Sutar H, Mishra SC, Sahoo SK, Acharya SK. Dry sliding wear behavior of Aluminium matrix composite using red mud an industrial waste. *International Research Journal of Pure & Applied Chemistry* 2013; **3** (1): 59-74.

[17] ASTM. Standard test method for water absorption, bulk density, apparent porosity, and apparent specific

gravity of fired whiteware products. *ASTM Standards, Vol 1502* 2006: 122-123.

[18] Boopathi MM, Arulshri K, Iyandurai N. Evaluation of mechanical properties of Aluminium alloy 2024 reinforced with silicon carbide and fly ash hybrid metal matrix composites. *American Journal of Applied Sciences* 2013; **10** (3): 219-229.

[19] Hashim J, Looney L, Hashmi M. Metal matrix composites: production by the stir casting method. *Journal of Materials Processing Technology* 1999; **92**: 1-7.

[20] Alaneme KK. Mechanical behaviour of cold deformed and solution heat-treated Alumina reinforced AA 6063 metal matrix composites. *The West Indian Journal of Engineering* 2013; **35** (2): 31-35.

[21] Alaneme KK, Anabaranze YO, Oke SR. Softening resistance, dimensional stability and corrosion behavior of alumina and rice husk ash reinforced Aluminum matrix composites subjected to thermal cycling. *Tribology in Industry* 2015; **37** (2): 204-214.

[22] Ramezanianpour A, Mahdikhani M, Ahmadibeni G. The effect of rice husk ash on mechanical properties and durability of sustainable concretes. *International Journal of Civil Engineering* 2009; **7** (2): 83-91.

[23] Onojah A, Agbendeh N, Mbakaan C. Rice husk ash refractory: the temperature dependent crystalline phase aspects. *International Journal of Recent Research and Applied Studies* 2013; **15** (2): 246-248.

[24] Aigbodion VS. Development of Al-Si-Fe/Rice husk ash particulate composites synthesis by double stir casting method. *Usak University Journal of Material Sciences* 2012; **1** (2): 187-197.

[25] Abdizadeh H, Ebrahimifard R, Baghchesara MA. Investigation of microstructure and mechanical properties of nano MgO reinforced Al composites manufactured by stir casting and powder metallurgy methods: A comparative study. *Composites Part B: Engineering* 2014; **56**: 217-221.

[26] Sharma R, Sharma P, Singh G. Dry sliding behavior of Aluminium alloy reinforced with hybrid ceramic particles. *International Journal of Multidisciplinary Research and Development, India* 2015; **2** (10): 485-491.

[27] Prasad DS, Krishna AR. Tribological properties of A356. 2/RHA composites. *Journal of Materials Science & Technology* 2012; **28** (4): 367-372.

[28] Kumar SJ, et al. Mechanical and dry sliding wear behavior of Al6063/Al2O3/Graphite hybrid composites. *International Journal of Innovative Research in Science, Engineering and Technology* 2014; **3** (3): 1222-1228.

[29] Nurani SJ, Saha CK. Aluminium composites and further improvement in their tribological properties-A review. *Journal of Modern Science and Technology* 2015; **3** (1): 183-192.

[30] Anilkumar A, Anilkumar C, Reddappa H. Studies on mechanical, wear and corrosion properties of Al6061-beryl-cerium oxide hybrid metal matrix composites. *Wear* 2014;.

[31] Singh KK, Singh S, Shrivastava AK. Study on tribological behavior of silicon carbide based. Advances in Materials Science and Engineering 2016; ID 3813412: 11 pp.

[32] Suresh R, Kumar MP. Investigation of tribological behavior and its relation with processing and microstructures of Al 6061 metal matrix composites. *International Journal of Research in Engineering & Technology* 2013; **1** (2): 91-104.